Elastic properties of cubic and rhombohedral $BiFeO_3$ from first-principles calculations

S. L. Shang,* G. Sheng, Y. Wang, L. Q. Chen, and Z. K. Liu
Department of Materials Science and Engineering, The Pennsylvania State University, University Park, Pennsylvania 16802, USA
(Received 24 March 2009; revised manuscript received 19 May 2009; published 18 August 2009)

First-principles elastic constants c_{ij}'s of $BiFeO_3$ with cubic nonmagnetic (NM)/ferromagnetic (FM) structures and rhombohedral antiferromagnetic (AFM) structure have been calculated within the generalized gradient approximation (GGA) and the GGA+U approach. In addition, the elastic properties of polycrystalline aggregates including bulk modulus and shear modulus are also determined and compared with experiments. It is found that the predicted c_{ij}'s decrease with increasing volume (or decreasing pressure) except for the c_{14} of the rhombohedral AFM phase. The cubic NM and FM phases are predicted to be harder than the rhombohedral AFM one, indicated by their smaller equilibrium volumes and larger bulk moduli. Additionally, the cubic FM phase is found nearly isotropy (by GGA and GGA+U with $U_{\text{eff}}=6$ eV), and the cubic NM phase is mechanical unstable at high temperatures. The presently predicted c_{ij}'s of $BiFeO_3$ provide helpful guidance for future measurements, and make the stress estimation and elastic energy calculation in $BiFeO_3$ thin films possible.

DOI: 10.1103/PhysRevB.80.052102 PACS number(s): 62.20.D−, 71.15.Mb, 75.50.Ee, 77.80.−e

$BiFeO_3$ is the only known material possessing simultaneously ferroelectric and magnetic orders at room temperature.[1–4] It is a rhombohedrally distorted ferroelectric perovskite with space group $R3c$ below the Curie temperature ($T_C \approx 1110$ K), and shows G-type canted antiferromagnetism (AFM) up to Néel temperature ($T_N \approx 643$ K).[5] These unique multiferroic properties make $BiFeO_3$ attracting great interest for potential applications in novel magnetoelectric devices and fuel considerable theoretical and experimental researches, especially in thin-film cases.[6] Despite the abundant research on $BiFeO_3$, relatively little is known regarding its elastic properties. Only the bulk modulus of the G-type rhombohedral (Rho) AFM phase (space group $R3c$) was measured based on the high-pressure data,[7] and the first-principles elastic constants[8] of the undistorted cubic ferromagnetic (FM) phase (space group $Pm\bar{3}m$) were predicted in terms of the local-density approximation (LDA).[9] Until now the elastic constants are unknown for the rhombohedral AFM phase from either experiments or predictions, which inhibits the fundamental understanding and fabrication of $BiFeO_3$, for instance, the stress analysis[10] and strain energy estimation[11] in epitaxial thin films, and the phase-field simulation including elastic energy.[8,12] The dearth of elastic properties in $BiFeO_3$ therefore motivates the present research.

The present work aims at getting insight into the first-principles elastic properties of $BiFeO_3$ with undistorted cubic nonmagnetic (NM) and FM structures (space group $Pm\bar{3}m$) and distorted G-type rhombohedral AFM structure (space group $R3c$). The study of cubic NM phase is due to its occurrence around 1200 K,[13] and is definitely paraelectric or paramagnetic. To these ends, an effective stress vs strain method as described in Ref. 14 is employed to calculate the elastic constants c_{ij}'s of $BiFeO_3$ with VASP code[15] as the computational engine. The electron-ion interaction is described via the projector augmented wave method by considering its accuracy with respect to the all-electron method and its efficiency as compared with ultrasoft pseudopotential method.[16] The generalized gradient approximation (GGA), Ref. 17, instead of LDA is adopted herein to depict the exchange-correction functional, since GGA predicts more accurate structural properties of $BiFeO_3$ (see, e.g., Refs. 18 and 19), which are of crucial importance in the calculation of elastic constants. Although Ravindran *et al.*[18] indicated that the structural and magnetoelectric properties of $BiFeO_3$ can be depicted well by GGA, ancillary calculations using the GGA+U approach are also performed for magnetic phases (cubic FM and rhombohedral AFM) in order to take into account the strong on-site Coulomb interaction (U) presented in the localized $3d$ electrons of Fe, and in turn to describe well the optical properties (e.g., band gap) and magnetic interaction. It is worth mentioning that the GGA+U (or LDA+U) method as implemented in VASP introduces magnetism, we therefore did not perform GGA+U calculations for cubic NM phase. In the present work, the GGA+U of Dudarev *et al.*[20] is used, which depends on the effective Coulomb interaction $U_{\text{eff}}=U-J$, with J being the screened exchange energy. In the first-principles calculations, we employ a plane-wave energy cutoff of 520 eV and k-point samplings of $11\times11\times11$ (for rhombohedral AFM phase) and $20\times20\times20$ (for cubic phases). The electronic energies are convergent to at least 0.001 meV/atom, and all force components are relaxed to at least 2 meV/Å. The relaxations of cell shape and ions' positions are performed by the Gaussian smearing technique. Note that only the ion's positions are relaxed in the calculations of elastic constants for rhombohedral AFM phase. Afterwards, the final total energy and elastic constants are determined on the relaxed structures by using the tetrahedron method incorporating Blöchl corrections.[21]

As an example, Fig. 1 illustrates the GGA-calculated total energies and magnetic moments of the cubic NM/FM phases and the rhombohedral AFM phase as a function of volume. The magnetic moments of the cubic FM phase show increasing trends with increasing volume, while the (site-projected) magnetic moments of Fe in rhombohedral AFM phase increase slightly and agree with the low-temperature measurement of $3.75\mu_B$ from neutron diffraction.[22] Figure 1 also shows that the total energy of the rhombohedral AFM phase is 0.185 and 0.303 eV/atom (by GGA) lower than those of the cubic FM and NM phases, respectively, indicating the ground state of $BiFeO_3$ is the rhombohedral AFM phase. The energy vs volume curves shown in Fig. 1 are the fittings by the four-parameter Birch-Murnaghan equation of state (EoS),[23]

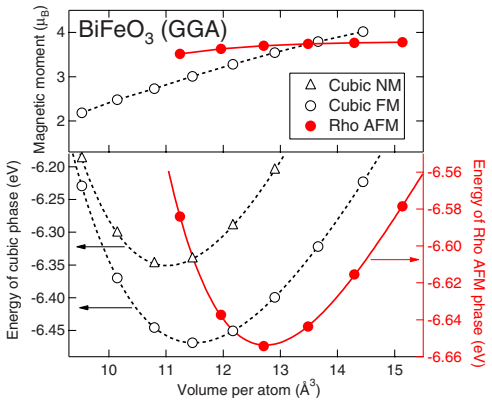

FIG. 1. (Color online) GGA-calculated total energies and magnetic moments of Fe (the site-projected values are shown for AFM phase) for cubic NM/FM and Rho AFM $BiFeO_3$ as a function of volume. The energy vs volume curves are fitted by the Birch-Murnaghan EoS as shown in Eq. (1).

$$E(V) = a + bV^{-2/3} + cV^{-4/3} + dV^{-6/3}, \tag{1}$$

where V is the volume, a, b, c, and d are the fitting parameters. The EoS predicted equilibrium properties are given in Table I, including volume V_0, bulk modulus B_0, and its pressure derivative B_0'. The predicted bulk moduli of rhombohedral AFM phase (89–101GPa, see Table I) agree with the room-temperature measurement of 75.5 ± 15.5 GPa.[7] It is worth mentioning that we do not consider the influences of temperature and zero-point vibrational energy, which will, in general, decrease the bulk modulus. For the rhombohedral AFM phase, previous predictions of bulk moduli are 130.9 GPa by GGA[18] and 130 GPa by LDA,[24] which are obviously larger than the experiment.[7] Regarding the V_0 of rhombohedral AFM phase, the present prediction ($\sim$12.74 Å^3 per atom by GGA) is slightly larger than the measured 12.46 Å^3 per atom,[5] and it is better than the prediction by LDA (11.6 Å^3 per atom).[2] For cubic phases, the FM order has lower bulk modulus and larger volume than those of the NM one due to the influence of magnetism. We also find that the cubic phases (both FM and NM) are harder than the AFM phase indicated by the equilibrium volumes [e.g., 11.49(11.02) Å^3/atom vs 12.74 Å^3/atom by GGA as shown in Table I]. Regarding the GGA+U, it predicts the similar structural properties as by GGA (see Table I), but the GGA+U predicts correctly the band gap of the rhombohedral AFM phase with $U_{\text{eff}}=6$ eV: i.e., 2.38 eV vs the measured 2.4–2.74 eV.[4,25,26] For cubic FM phase, the GGA+U will predict a metal when $U_{\text{eff}}<3$ eV, and an insulator when $U_{\text{eff}}>3$ eV (see Table I). We also note that U_{eff} can, in fact, be computed in a self-consistent way based on the approach of Cococcioni and de Gironcoli[27] (for example), and Kornev *et al.*[3] reported the $U_{\text{eff}}=3.8$ eV for LDA+U [the U_{eff} value should be smaller for GGA+U (Ref. 28)]. However, we were able to make a suitable choice of U_{eff} based on experimental data (band gap herein). Note that there is no magic U_{eff} which reproduces everything together (e.g., band gap and magnetic interaction). Therefore, the present choices of $U_{\text{eff}}=3$ and 6 eV consider (i) the measured band gaps of $BiFeO_3$ and (ii) the commonly used U_{eff} values (2–6 eV) in previous first-principles calculations by GGA+U or LDA+U.[3,19,29–31]

The GGA and GGA+U predict elastic constants c_{ij}'s are shown in Table I for cubic ($Pm\bar{3}m$) NM and FM, and rhombohedral ($R3c$) AFM $BiFeO_3$. Wherein the predictions are mainly based on the strains $x=\pm 0.01$ (ancillary strains of ± 0.007 and ± 0.013 are also tested, and we found the elastic errors are less than 1%), and the following six sets of linearly independent strain vectors:[14]

$$\begin{pmatrix} x & 0 & 0 & 0 & 0 & 0 \\ 0 & x & 0 & 0 & 0 & 0 \\ 0 & 0 & x & 0 & 0 & 0 \\ 0 & 0 & 0 & x & 0 & 0 \\ 0 & 0 & 0 & 0 & x & 0 \\ 0 & 0 & 0 & 0 & 0 & x \end{pmatrix}. \tag{2}$$

Based on the strain vectors in Eq. (2), the first-principles-predicted stress vectors, and the general Hooke's law, the c_{ij}'s are determined (see details in Ref. 14). As shown in Table I, with increasing U_{eff}, c_{11} (c_{33}) and c_{44} increase, c_{12} (c_{14}) decrease, while c_{13} keeps constant. The GGA (i.e., $U_{\text{eff}}=0$ eV) predicted c_{ij}'s are also shown in Fig. 2 as a function of volume. Except for the c_{14} of the rhombohedral AFM phase, all the c_{ij}'s decrease with increasing volume (or decreasing pressure). Previous LDA predictions of the cubic FM phase give $c_{11}=302$ GPa, $c_{12}=162$ GPa, and $c_{44}=68$ GPa,[8] which are quite close to the present results at the lower volume of 10.8 Å^3 per atom (see Fig. 2), since LDA predicts lower equilibrium volume with respect to GGA. Figure 2 shows that the cubic NM phase is mechanically unstable due to the elastic energy must be positive, i.e., the c_{ij} matrix should satisfy the Born stability criteria.[32] When the volume of cubic NM phase is slightly larger than the equilibrium one, $c_{11}<c_{12}$ happens, indicating the NM phase is unstable at high temperatures. We therefore conclude that the cubic NM phase cannot represent the cubic paramagnetic phase occurring at high temperatures (>1200 K). Instead, the cubic paramagnetic phase should be represented by a mixture of different magnetic configurations. Figure 2 also shows that the rhombohedral AFM phase is mechanically unstable at larger volumes based on the Born stability criteria.[32] For a rhombohedral structure, they are

$$c_{11} - |c_{12}| > 0, \tag{3a}$$

$$(c_{11} + c_{12})c_{33} - 2c_{13}^2 > 0, \tag{3b}$$

$$(c_{11} - c_{12})c_{44} - 2c_{14}^2 > 0. \tag{3c}$$

According to Eq. (3c), the AFM phase is predicted (by GGA) to be elastic instability when its volume greater than 13.35 Å^3/atom, due to the decrease in c_{44} and the increase in c_{14}. This instability could hint at a ferroelastic phase transition[33] or melting[34] achieved at high temperatures or at negative pressures (such as in thin-film cases).

Based on the predicted c_{ij}'s, the corresponding bulk modulus and shear modulus can be calculated in terms of Voigt-Reuss-Hill approach.[35] Note that the Voigt, Reuss, and Hill bulk moduli are identical for any cubic phase. As shown in Table I, for the rhombohedral AFM phase the obtained bulk moduli from c_{ij}'s are larger than the ones from EoS fittings by 5–10%, since (i) the energy vs volume points used

TABLE I. Calculated (by GGA, i.e., $U_{\text{eff}}=0$ eV, and GGA+U) and experimental properties of $BiFeO_3$ with cubic FM/NM and G-type Rho AFM structures, including the equilibrium volume V_0 (Å^3/atom), bulk modulus B_0 (GPa for elastic properties), and its pressure derivative B_0' by EoS of Eq. (1), single-crystal elastic constants c_{ij}, polycrystal aggregate properties of bulk modulus (B) and shear modulus (G) in Voigt-Reuss-Hill approaches, the B/G ratio in Hill approach, the anisotropy ratios (A), and the band gap (eV).

	U_{eff} (Rho AFM)			U_{eff} (Cubic FM and NM[a])		
Property	0	3	6	0	3	6
V_0 (EoS)	12.74	12.77	12.66	11.49 (11.02)	12.19	12.08
B_0 (EoS)	89	96	101	160 (196)	153	163
B_0' (EoS)	7.66	7.82	7.66	4.73 (4.71)	3.49	4.25
c_{11}	203	213	222	229 (195)	228	279
c_{12}	117	111	110	123 (191)	128	108
c_{13}	50	49	50			
c_{14}	23	19	16			
c_{33}	129	139	150			
c_{44}	31	39	49	58 (62)	65	79
G_V	42	50	56	56 (38)	59	82
G_R	25	39	50	56 (4)	58	81
G_H	34	45	53	56 (21)	59	82
B_V	108	109	113	158 (193)	162	165
B_R	96	99	104	158 (193)	162	165
B_H	102	104	108	158 (193)	162	165
B_H/G_H	3.04	2.34	2.03	2.83 (9.15)	2.75	2.02
A_1	0.71	0.77	0.88	1.09 (34.87)	1.30	0.92
A_2	0.53	0.62	0.72			
A_G (%)	26.03	11.37	5.76	0.10 (79.79)	0.76	0.07
A_B (%)	5.74	4.86	4.14			
Band gap	0.95	1.92	2.38	None	~0	0.28
Band gap (Expt.)	2.4[b]					
	2.5[c]					
	2.74[d]					
V_0 (Expt.)	12.46[e]					
B_0 (Expt.)	75.5 ± 15.5 [f]					
B_0 (Calc.)	130.9[g]					
	130[h]					

[a]Results of cubic NM phase ($U_{\text{eff}}=0$ eV) are shown in the parentheses.
[b]Reference 25.
[c]Reference 26.
[d]Reference 4.
[e]Reference 5.
[f]Reference 7.
[g]First-principles prediction by GGA (Ref. 18).
[h]First-principles prediction by LDA (Ref. 24).

in the EoS fittings are not in the fully elastic region, unlike the determinations of c_{ij}'s and (ii) all the freedoms of crystal are allowed to relax, while the cell shape is fixed in the determination of c_{ij}'s. For the cubic phase, the obtained bulk moduli from EoS fittings and c_{ij}'s are close to each other, except for the $U_{\text{eff}}=3$ eV for cubic FM case due to the magnetic effects: the magnetic moments increase in low-volume region, but keep almost constant at high-volume region (not shown). For both rhombohedral AFM and cubic FM phases, with increasing U_{eff}, the bulk moduli and shear moduli increase, while the B/G (bulk modulus/shear modulus) ratios decrease from ~3 to ~2, but these B/G ratios are all greater than the "critical" value of 1.75, indicating the ductile nature of $BiFeO_3$, since a value of ~1.75 separates ductile and brittle materials according to Pugh criterion.[36]

Starting from the predicted c_{ij}'s, it is found that the anisotropy ratios of cubic FM phase ($U_{\text{eff}}=0$ and 6 eV) are close to unity, 1 (see Table I), based on the definition of $A_1=2c_{44}/(c_{11}-c_{12})$. The isotropy nature of cubic FM phase is comparable with the known near-isotropy materials of W, $SrTiO_3$, etc.[37] For the rhombohedral AFM phase, its anisotropy ratios are also shown in Table I with the definitions of $A_1=2c_{44}/(c_{11}-c_{12})=c_{44}/c_{66}$ and $A_2=4c_{44}/(c_{11}+c_{33}-2c_{13})$: the {100} shear planes between the ⟨011⟩ and ⟨010⟩ direc-

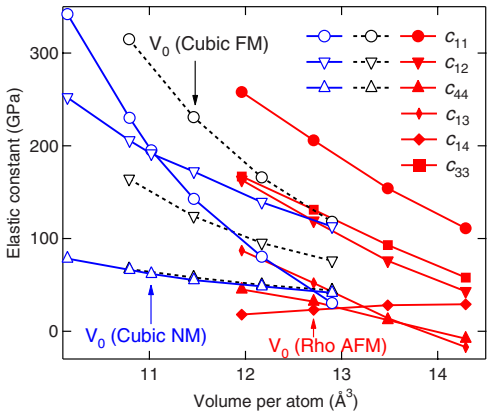

FIG. 2. (Color online) GGA-calculated elastic constants c_{ij}'s for cubic NM (open symbols with solid lines), cubic FM (open symbols with dashed lines), and G-type rhombohedral (Rho) AFM (filled symbols with solid lines) phases of $BiFeO_3$ as a function of volume.

tions for A_2.[38] The AFM phase is obviously anisotropy with respect to the cubic FM phase. Regarding the elastic anisotropy, Chung and Buessem[37] also proposed the general definitions based on the differences between B_V and B_R (the Voigt and Reuss values of bulk moduli, respectively) and between G_V and G_R,

$$A_B = (B_V - B_R)/(B_V + B_R) \tag{4a}$$

$$A_G = (G_V - G_R)/(G_V + G_R). \tag{4b}$$

Equations (4a) and (4b) indicate that the farther the values of A_B and A_G from zero, the larger the anisotropy of material. For isotropy materials $A_B = A_G = 0$. Note that only A_G is available for cubic phase due to $B_V = B_R$ in any cubic structure. Table I shows that the percent values of A_B and A_G for $BiFeO_3$, which also depict the isotropy nature of the cubic FM phase (U_{eff}=0 and 6 eV), but the anisotropy nature for the rhombohedral AFM phase. It is also found that, with increasing U_{eff} the anisotropy of the AFM phase decreases, indicating by the values of A_1 and A_2 more close to unity, 1, and the values of A_B and A_G decreasing. Regarding the elastic properties of cubic NM phase shown in Table I, they are for reference only since we think the cubic NM phase cannot represent the observed cubic paramagnetic phase at high temperatures[13] (see discussion above).

In summary, the elastic properties of $BiFeO_3$ with cubic NM/FM structures, and rhombohedral G-type AFM structure (i.e., the distorted cubic structure) have been calculated within the GGA approach and the ancillary GGA+U approach, and compared with available measurements/predictions. It is found that the predicted elastic constants c_{ij}'s decrease with increasing volume (or decreasing pressure) except for the c_{14} of the rhombohedral AFM phase. The cubic NM/FM phases are harder than the rhombohedral AFM phase, represented by the smaller equilibrium volumes and larger bulk moduli of cubic phases. The cubic FM phase is found nearly isotropy by GGA and GGA+U with U_{eff} =6 eV. The cubic NM phase is found mechanically unstable at high temperatures, and therefore cannot represent the observed cubic paramagnetic phase.

This work was funded by NSF through Grant No. DMR-0510180 and U.S. DOE Basic Sciences under Contract No. DE-FG02–07ER46417. First-principles calculations were carried out on the LION clusters at the Pennsylvania State University, and on the resources of NERSC, which is supported by the Office of Science of the U.S. DOE under Contract No. DE-AC02-05CH11231.

*sus26@psu.edu

[1] P. Fischer *et al.*, J. Phys. C **13**, 1931 (1980).
[2] J. Wang *et al.*, Science **299**, 1719 (2003).
[3] I. A. Kornev *et al.*, Phys. Rev. Lett. **99**, 227602 (2007).
[4] J. F. Ihlefeld *et al.*, Appl. Phys. Lett. **92**, 142908 (2008).
[5] F. Kubel and H. Schmid, Acta Crystallogr., Sect. B: Struct. Sci. **46**, 698 (1990).
[6] R. Ramesh and N. A. Spaldin, Nature Mater. **6**, 21 (2007).
[7] A. G. Gavriliuk *et al.*, Phys. Rev. B **77**, 155112 (2008).
[8] J. X. Zhang *et al.*, J. Appl. Phys. **101**, 114105 (2007).
[9] J. P. Perdew and A. Zunger, Phys. Rev. B **23**, 5048 (1981).
[10] T. Gressmann *et al.*, Acta Mater. **55**, 5833 (2007).
[11] J. Y. Shen *et al.*, J. Cryst. Growth **240**, 6 (2002).
[12] L. Q. Chen, Annu. Rev. Mater. Res. **32**, 113 (2002).
[13] R. Palai *et al.*, Phys. Rev. B **77**, 014110 (2008).
[14] S. L. Shang *et al.*, Appl. Phys. Lett. **90**, 101909 (2007).
[15] G. Kresse and J. Furthmuller, Comput. Mater. Sci. **6**, 15 (1996).
[16] G. Kresse and D. Joubert, Phys. Rev. B **59**, 1758 (1999).
[17] J. P. Perdew *et al.*, Phys. Rev. Lett. **77**, 3865 (1996).
[18] P. Ravindran *et al.*, Phys. Rev. B **74**, 224412 (2006).
[19] L. Bi *et al.*, Phys. Rev. B **78**, 104106 (2008).
[20] S. L. Dudarev *et al.*, Phys. Rev. B **57**, 1505 (1998).
[21] P. E. Blöchl *et al.*, Phys. Rev. B **49**, 16223 (1994).
[22] I. Sosnowska *et al.*, Appl. Phys. A: Mater. Sci. Process. **74**, S1040 (2002).
[23] S. L. Shang *et al.* (unpublished).
[24] O. E. González-Vázquez and J. Íñiguez, Phys. Rev. B **79**, 064102 (2009).
[25] T. P. Gujar *et al.*, Mater. Chem. Phys. **103**, 142 (2007).
[26] F. Gao *et al.*, Appl. Phys. Lett. **89**, 102506 (2006).
[27] M. Cococcioni and S. de Gironcoli, Phys. Rev. B **71**, 035105 (2005).
[28] S. Fabris *et al.*, Phys. Rev. B **71**, 041102(R) (2005).
[29] P. Baettig *et al.*, Phys. Rev. B **72**, 214105 (2005).
[30] H. M. Tutuncu and G. P. Srivastava, Phys. Rev. B **78**, 235209 (2008).
[31] M. Goffinet *et al.*, Phys. Rev. B **79**, 014403 (2009).
[32] M. Born and K. Huang, *Dynamical Theory of Crystal Lattices* (Oxford University Press, New York, 1988).
[33] P. Toledano *et al.*, Phys. Rev. B **27**, 5717 (1983).
[34] R. W. Cahn, Nature (London) **413**, 582 (2001).
[35] G. Simmons and H. Wang, *Single Crystal Elastic Constants and Calculated Aggregate Properties* (MIT, Cambridge, MA, 1971).
[36] S. F. Pugh, Philos. Mag. **45**, 823 (1954).
[37] D. H. Chung and W. R. Buessem, in *Anisotropy in Single Crystal Refractory Compounds*, edited by F. W. Vahldiek and S. A. Mersol (Plenum, New York, 1968), Vol. 2, p. 217.
[38] P. Ravindran *et al.*, J. Appl. Phys. **84**, 4891 (1998).